IEEE Access
Multidisciplinary | Rapid Review | Open Access Journal

Received January 14, 2020, accepted February 4, 2020, date of publication February 17, 2020, date of current version February 27, 2020.

Digital Object Identifier 10.1109/ACCESS.2020.2974240

Online Estimation and Control for Feed Drive Systems With Unmeasurable Parameter Variations

TIANCHENG ZHONG[1], RYOZO NAGAMUNE[2], (Senior Member, IEEE), ALEXANDER YUEN[2], AND WENCHENG TANG[1]

[1]School of Mechanical Engineering, Southeast University, Nanjing 211189, China
[2]Department of Mechanical Engineering, The University of British Columbia, Vancouver, BC V6T 1Z4, Canada

Corresponding author: Tiancheng Zhong (tianchengzhong@seu.edu.cn)

This work was supported in part by the National Natural Science Foundation of China under Grant 51675100, and in part by the National Science and Technology Major Projects under Grant 2013ZX04008011.

ABSTRACT This paper develops an online parameter estimation and control method for both rigid and flexible feed drive systems with unmeasurable parameter variations. The perturbations of the state-space model caused by the parameter variations are formulated, thereby making it possible to obtain the parameter variations in real-time by estimating the perturbations. To estimate the perturbations, they are regarded as the extended states and estimated through the extended-state-observer. With the estimation method, a novel state feedback control structure with double integrators is further proposed, which can eliminate the steady-state tracking error at constant velocities. The H_∞ optimization technique is used to design the proposed state feedback controller. A simulation is conducted that integrates the estimator and the controller for a ball screw setup with mass-dependent resonant modes, where several proposed state feedback controllers are linearly interpolated into a gain-scheduling controller and scheduled by the estimated mass. The results demonstrate that the designed gain-scheduling state feedback controller outperforms a linear-time-invariant state feedback controller and an adaptive backstepping sliding mode controller. The proposed method is experimentally validated on a rigid linear-motor-driven motion stage, of which the results indicate the proposed estimation method can accurately estimate the parameter variations.

INDEX TERMS Extended-state-observer, feed drive systems, H_∞ optimization, parameter estimation, state feedback control.

I. INTRODUCTION

The rapidly developing high-speed machining requires fast and accurate feed drive systems. However, the performances of feed drive systems are commonly limited by resonant modes [1], which can be excited by external disturbances, such as the cutting force, during high-speed machining. To achieve satisfactory performances, various advanced control methods have been applied to feed drive systems, e.g., sliding mode control [2], state feedback control, including pole placement [3] and linear quadratic regulator [4], additional feedback loop control [5], H_∞ robust control [6], and active disturbance rejection control [7]. These methods can improve the tracking performance, but they are commonly designed for the nominal model, of which the parameters are varying during the machining processes. Once the parameter values change, the performance and the stability of feed drive control systems based on the nominal model may be degraded.

Some control methods have been studied for feed drive systems, which take into account the impacts of parameter variations, such as load mass and stiffness change. Furthermore, two types of gain-scheduling control were applied to feed drive systems with table-position-dependent dynamics: the linear-parameter-varying (LPV) method [6], [8], [9] and interpolating method [10], [11]. For the same purpose, the neural network was also studied to interpolate the resonant filter parameters [12]. Nevertheless, it is still challenging to employ the varying parameters as gain-scheduling parameters if they are not measurable in real-time. Although some

The associate editor coordinating the review of this manuscript and approving it for publication was Engang Tian.

methods can consider variations in the unmeasurable parameters by regarding them as uncertainties and design either robust linear-time-invariant (LTI) controller [13] or advanced gain-scheduling controller [14], these methods can not avoid the inherent conservatism that will limit the performances of control systems.

The adaptive control and the learning control can be used to consider the unmeasurable parameter variations. For instance, adaptive control and robust control were combined into the adaptive robust control to consider the parameter uncertainties [15]. This method was further integrated with the linear extended-state-observer for DC motor control [16]. The adaptive control was also used in the feedforward framework for vibration suppression [17]. Furthermore, the adaptive control was widely used in the sliding mode control for feed drive systems [18]–[22]. Although the adaptive control can handle the unmeasurable parameter variations, it is commonly used in the specific control framework and can not obtain the exact parameter variations. On the other hand, the learning control was studied on a ball-screw-driven-stage for the repetitive tasks [23]. This method can achieve high-precision positioning, while its effectiveness will be affected for varying tasks.

As a summary, limited control methods can adequately handle the impacts of parameter variations on the control performances in feed drive systems due to the unmeasurable feature. Therefore, it is crucial to develop an online parameter estimation method to detect the unmeasurable parameter variations and address their impacts by updating the controller. Some methods of parameter estimation were proposed for servomotors in the discrete domain, which were based on the disturbance-observer [24], [25]. However, the iterations are necessary to obtain accurate estimation results, and the relationship between the observed output and the parameter variations is not explicitly obtained. Furthermore, these methods were proposed only for the rigid model but not for the flexible model. These drawbacks will be improved by the online parameter estimation proposed in this paper.

The objective of this paper is to develop integrated online estimation and control that estimate the parameter variations in real-time and update the controller using the estimated parameters. Motivated by the parameter estimation with finite-time convergence [26] and inspired by the principle of generalized extended-state-observer [27], a parameter estimation method is developed for both rigid and flexible feed drive systems. Furthermore, concerning the controller design, the conventional structure of state feedback servo control used in [3], [4] yields the steady-state error for the ramp input, which means the tracking error exists at constant velocities. Although the feedforward loop can reduce the tracking error at constant velocities, it highly depends on the model accuracy, and the parameter variations would damage the effectiveness of the feedforward loop. Therefore, a novel state feedback control structure is proposed for feed drive systems to eliminate tracking error of conventional state feedback servo control at constant velocities.

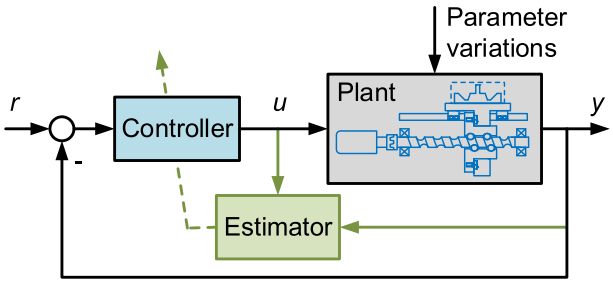

FIGURE 1. Configuration of feed drive control systems.

The main contribution of this work consists of two aspects: formulating the perturbations caused by the parameter variations, and proposing a state feedback control structure with the double integrators. By formulating the perturbations, the parameter variation can be obtained in real-time by estimating the perturbations. To estimate the perturbations, they are regarded as the extended states and estimated through the extended-state-observer [27], [28]. On the other hand, the proposed control structure skillfully includes an additional integrator, which eliminates the tracking error at constant velocities and makes it available to design the proposed state feedback controller through existing optimization methods. The H_∞ performance has been used to design the controller [29], [30], and is adopted to optimize the state feedback controller in this paper.

In the proposed estimation and control framework, the estimated parameters can be used to update the controller, thereby circumventing the performance degradation introduced by the parameter variations. The extensive simulation and experiment indicate the proposed parameter estimation method can accurately obtain the parameter variations, and the impacts of the unmeasurable parameter variations can be well compensated by using the estimated parameter to schedule the controller gain.

II. PRELIMINARIES

The standard control system of feed drives is shown in Fig. 1, in black arrows and black blocks. After applying the trajectory r to the system, the error between the trajectory r and the table position y is input to the controller. Accordingly, the controller outputs the voltage u to the motor, which generates the torque to drive the table through the transmission mechanism.

A. PARAMETER VARIATIONS AND SOLUTION

During machining processes, some model parameters are not constant but varying. For instance, the workpiece material is removed from workpieces in cutting processes or increased in additive manufacturing processes. The different workpiece mass may cause the change of the equivalent mass over 100%. Furthermore, the viscous friction coefficient may also change due to the lubrication condition, thereby affecting the equivalent viscous friction coefficient.

These parameter variations may deteriorate the control performance and even destroy the closed-loop stability [10]. For instance, the effectiveness of acceleration feedforward control requires the accurate value of the equivalent mass, and the friction compensation is influenced by the equivalent viscous friction coefficient. Besides, the variation in workpiece mass would change the natural frequency of the flexible feed drive systems, thereby degrading the vibration control performance and reducing the stability margin.

A common challenge of these parameter variations is that they are not directly measurable. As a result, the control system cannot handle its effects. To overcome the effects, an integrated strategy of online parameter estimation and control is developed in this paper. As shown in the green block of Fig. 1, an estimator is proposed to obtain the parameter variations in real-time, and then the estimated parameters can be used to update the controller.

B. MODELS OF FEED DRIVE SYSTEMS

The various feed drive systems can be mainly modeled in two types: the rigid model and the flexible model.

1) RIGID MODEL

Many types of feed drive systems, including the servo motor and the linear motor, can be modeled by the rigid body motion. With the lumped model, the corresponding state-space equations are given as

$$\begin{cases} \dot{p} = v, \\ \dot{v} = (-bv + u)/m, \\ y = p, \end{cases} \tag{1}$$

where the system states $\boldsymbol{x}_p$ consist of the table position p and the table velocity v, and the control input u is the motor voltage. The model parameters m and b denote the equivalent mass and the equivalent viscous friction coefficient, respectively, which are varying during the machining processes.

2) FLEXIBLE MODEL

For the feed drive systems with the resonant modes, such as ball screw drives, the flexible model can be built as the two-degree-of-freedom model, which regards the transmission between the motor and the table as a spring-damper structure. Accordingly, the state-space equations with system states $\boldsymbol{x}_p = [p_1 \;\; p_2 \;\; v_1 \;\; v_2]^T$ are given as follows:

$$\begin{cases} \dot{p_1} = v_1, \\ \dot{v}_1 = [-kp_1 + kp_2 - (c + b_1)v_1 + cv_2 + u]/m_1, \\ \dot{p_2} = v_2, \\ \dot{v}_2 = [kp_1 - kp_2 + cv_1 - (c + b_2)v_2]/m_2, \\ y = p_2, \end{cases} \tag{2}$$

where k is the stiffness, and c is the damping coefficient. Subscript 1 and 2 denote the motor side and the table side, respectively.

For the flexible model, the equivalent viscous friction coefficient may change due to the varying lubrication, while the equivalent mass is affected by the workpiece mass. Since the workpiece is placed on the table side, the motor side equivalent mass m_1 is constant. Moreover, the stiffness k and the damping coefficient c depend on the table position, which can be directly measured by the encoder. Therefore, the variations in these parameters are ignored in this work.

III. PARAMETER ESTIMATION

A. THE PERTURBATIONS CAUSED BY PARAMETER VARIATIONS

1) PARAMETER VARIATIONS IN THE RIGID MODEL

Once the parameters m and b in the rigid model change, denoted by the symbol δ, the acceleration term $\dot{v}$ in the state-space equations (1) is perturbed as

$$\dot{v} = [-(b + \delta_b)v + u]/(m + \delta_m), \tag{3}$$

which can be transformed into

$$\dot{v} = [-bv + u - \delta_b v - \delta_m \dot{v}]/m. \tag{4}$$

By comparing (1) and (4), the parameter variations cause a perturbation

$$\boldsymbol{x}_c := -\delta_b v - \delta_m \dot{v}. \tag{5}$$

The bold font denotes the state and the perturbation in this paper. With the system states $\boldsymbol{x}_p$ and the extracted perturbation $\boldsymbol{x}_c$, the perturbed state-space model can be expressed as

$$\begin{cases} \dot{\boldsymbol{x}}_p = A_p \boldsymbol{x}_p + B_p u + B_c \boldsymbol{x}_c, \\ y = C_p \boldsymbol{x}_p, \end{cases} \tag{6}$$

where the matrices

$$A_p = \begin{bmatrix} 0 & 1 \\ 0 & -\frac{b}{m} \end{bmatrix}, \quad B_p = \begin{bmatrix} 0 \\ \frac{1}{m} \end{bmatrix}, \quad B_c = \begin{bmatrix} 0 \\ \frac{1}{m} \end{bmatrix}, \quad C_p = \begin{bmatrix} 1 & 0 \end{bmatrix}. \tag{7}$$

2) PARAMETER VARIATIONS IN THE FLEXIBLE MODEL

The perturbation derivation for the flexible model is analogous to the one for the rigid model. As mentioned in Section II-B, the equivalent mass m_2 and the equivalent viscous friction coefficient b_1 and b_2 may change during the machining processes. Therefore, the acceleration terms $\dot{v}_1$ and $\dot{v}_2$ in the state-space equations (2) are given by

$$\begin{cases} \dot{v}_1 = [-kp_1 + kp_2 - (c + b_1)v_1 + cv_2 + u - \delta_{b_1} v_1]/m_1, \\ \dot{v}_2 = [kp_1 - kp_2 + cv_1 - (c + b_2)v_2 - \delta_{b_2} v_2 - \delta_{m_2} \dot{v}_2]/m_2. \end{cases} \tag{8}$$

Compared to the state-space equations (2), the perturbations associated with the parameter variations occur on both sides of the motor and the table. By defining the perturbations as

$$\boldsymbol{x}_c := \begin{bmatrix} x_{c1} \\ x_{c2} \end{bmatrix} = \begin{bmatrix} -\delta_{b_1} v_1 \\ -\delta_{b_2} v_2 - \delta_{m_2} \dot{v}_2 \end{bmatrix} \tag{9}$$

the state-space matrices in (6) for the flexible model can be derived as

$$A_p = \begin{bmatrix} 0 & 1 & 0 & 0 \\ -\frac{k}{m_1} & -\frac{c+b_1}{m_1} & \frac{k}{m_1} & \frac{c}{m_1} \\ 0 & 0 & 0 & 1 \\ \frac{k}{m_2} & \frac{c}{m_2} & -\frac{k}{m_2} & -\frac{c+b_2}{m_2} \end{bmatrix}, \quad B_p = \begin{bmatrix} 0 \\ \frac{1}{m_1} \\ 0 \\ 0 \end{bmatrix},$$
$$B_c = \begin{bmatrix} 0 & 0 \\ \frac{1}{m_1} & 0 \\ 0 & 0 \\ 0 & \frac{1}{m_2} \end{bmatrix}, \; C_p = \begin{bmatrix} 0 & 0 & 1 & 0 \end{bmatrix}. \tag{10}$$

By seeing (5), the variation in equivalent viscous friction coefficient δ_b can be obtained by enforcing the feed drive system to operate in any constant speed v, i.e., $\dot{v} = 0$, as

$$\delta_b = \frac{-\boldsymbol{x}_c}{v}, \tag{11}$$

provided that the signal x_c is available. On the other hand, the variation in equivalent mass δ_m is found when the feed drive system changes its moving direction, i.e., $v = 0$, as

$$\delta_m = \frac{-\boldsymbol{x}_c}{\dot{v}}, \tag{12}$$

again with the provision of x_c's availability. An analogous argument holds for (9). Therefore, since the velocity v and acceleration $\dot{v}$ are measurable in feed drive systems, the estimation problem of parameter variations δ_b and δ_m is reduced to the problem of estimating the perturbation $\boldsymbol{x}_c$. Our approach for this reduced problem is the extended-state-observer, to be presented next.

B. PERTURBATION ESTIMATION THROUGH EXTENDED-STATE-OBSERVER

In this section, the perturbations will be estimated by using the extended-state-observer. To estimate the perturbations, they are regarded as the extended states, and the extended state-space model of the new system states $\boldsymbol{x}_e = [\boldsymbol{x}_p^T \;\; \boldsymbol{x}_c^T]^T$ can be obtained accordingly:

$$\begin{cases} \dot{\boldsymbol{x}}_e = A_e \boldsymbol{x}_e + B_e u + E\dot{\boldsymbol{x}}_c, \\ y = C_e \boldsymbol{x}_e, \end{cases} \tag{13}$$

where the extended state-space matrices are defined as

$$A_e := \begin{bmatrix} A_p & B_c \\ \mathbf{0}_{r\times n} & \mathbf{0}_{r\times r} \end{bmatrix}, \quad B_e := \begin{bmatrix} B_p \\ \mathbf{0}_{r\times 1} \end{bmatrix}, \quad E := \begin{bmatrix} \mathbf{0}_{n\times r} \\ I_{r\times r} \end{bmatrix},$$
$$C_e := \begin{bmatrix} C_p & \mathbf{0}_{1\times r} \end{bmatrix}.$$

The subscripts n and r denote the numbers of the plant states and the perturbations, respectively.

After regarding the perturbations as the extended states, the state observer can be designed for the extended system to estimate the extended states. Given the extended state-space model (13), the generalized extended-state-observer can be designed as:

$$\dot{\hat{\boldsymbol{x}}}_e = A_e \hat{\boldsymbol{x}}_e + B_e u + L(y - C_e \hat{\boldsymbol{x}}_e) \tag{14}$$

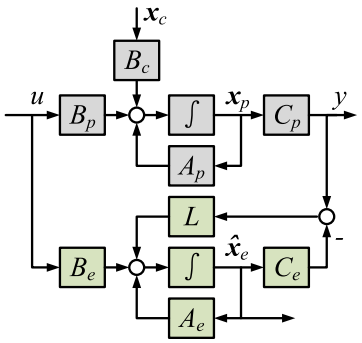

FIGURE 2. Configuration of the generalized extended-state-observer.

where $\hat{\boldsymbol{x}}_e = [\hat{\boldsymbol{x}}_p \;\; \hat{\boldsymbol{x}}_c]^T$ are the estimation states, and L includes the tuning parameters of the generalized extended-state-observer. The structure of the extended-state-observer is shown in Fig. 2.

C. ESTIMATION ERROR ANALYSIS

The estimation error is defined as $\boldsymbol{e}_x := \boldsymbol{x}_e - \hat{\boldsymbol{x}}_e$, and the state-space representation for the estimation error $\boldsymbol{e}$ is obtained by subtracting (13) from (14):

$$\dot{\boldsymbol{e}}_x = (A_e - LC_e)\boldsymbol{e}_x + E\dot{\boldsymbol{x}}_c \tag{15}$$

The time-domain solution of the state-space model (15) is given by

$$\boldsymbol{e}_x(t) = e^{(A_e - LC_e)t} e(0) + \int_0^t e^{(A_e - LC_e)(t-\tau)} E\dot{\boldsymbol{x}}_c d\tau, \tag{16}$$

where the symbol $e^{(\cdot)}$ denotes the matrix exponential term. For feed drive systems, the parameters would not vary arbitrarily fast but may change suddenly at some moment. For instance, the load mass may decrease once the weight is taken away in a pick-and-place machine. Assuming the parameters are steady during the estimation, the perturbation derivative for the rigid model is obtained according to (5):

$$\dot{\boldsymbol{x}}_c = -\delta_b \dot{v} - \delta_m \ddot{v}. \tag{17}$$

Given the perturbation derivative (17), the estimation error (16) for a linear trajectory can be discussed as two parts:

- If the velocity of feed drive systems is constant, i.e., $v \neq 0$ and $\dot{v} = \ddot{v} = 0$, the perturbation derivative $\dot{\boldsymbol{x}}_c = 0$, and the second term of (5) is zero. Therefore, the estimation error $\boldsymbol{e}_x$ will go to zero eventually, and the variation in the equivalent viscous friction coefficient can be accurately obtained at constant velocities.
- When feed drive systems are operated at constant acceleration, i.e., $v \neq 0$, $\dot{v} \neq 0$ and $\ddot{v} = 0$, the estimation error exist due to $\dot{\boldsymbol{x}}_c = -\delta_b \dot{v}$. However, if the feed drive system is operated with a small absolute value of acceleration $|\dot{v}|$, the estimation error $\boldsymbol{e}_x$ would be small enough and can be ignored as long as the eigenvalues of $(A_e - LC_e)$ are far away from the imaginary axis.

It is straightforward to derive similar conclusions for the flexible model.

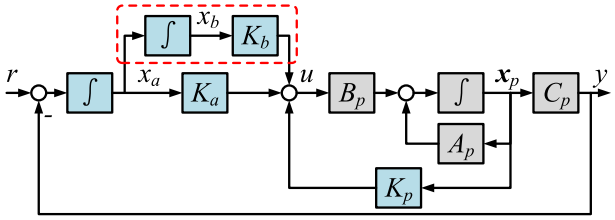

FIGURE 3. Configuration of the state feedback controller with double integrators.

D. PARAMETERIZATION OF PARAMETER ESTIMATOR

For the rigid model (1), the extended-state-observer (14) can be tuned by the bandwidth-based approach [31] to simplify the parameterization process. The tuning parameters can be designed as

$$L = [3\omega_e \;\; 3\omega_e^2 \;\; \omega_e^3]^T, \tag{18}$$

where ω_e is the desired observer bandwidth. For the flexible model (2), the extended-state-observer (14) can be designed through the pole-placement technique. To guarantee faster dynamics, the poles of the observer should be placed further from the imaginary axis than those of the closed-loop control system.

It should be noted that, although the larger observer bandwidth and the far poles contribute to the faster convergence and the smaller estimation error, the observer may capture the measurement noises existing in practices, thereby resulting in an inaccurate estimation.

IV. STATE FEEDBACK CONTROLLER DESIGN

Since the parameter estimator also estimates states of the initial state-space model, the state feedback controller can be employed. In this section, a state feedback control structure with the double integrators is presented, and the controller is designed through the H_∞ optimization.

A. STATE FEEDBACK CONTROL WITH DOUBLE INTEGRATORS

The configuration of the proposed state feedback control method is shown in Fig. 3. As shown in the red dashed block, the proposed control structure introduces a new state x_b:

$$\dot{x}_b = x_a. \tag{19}$$

Compared with the conventional structure of state feedback with an integrator, the effect of the introduced state x_b is to add another integrator to the open-loop system, thereby increasing the order of open-loop system type and eliminating the steady-state error at constant velocities.

Given the proposed control structure, the closed-loop state-space model with respect to the new system states $\boldsymbol{x} := [\boldsymbol{x}_p^T \;\; x_a \;\; x_b]^T$ is formulated accordingly:

$$\begin{cases} \dot{\boldsymbol{x}} = A\boldsymbol{x} + B_u u + B_r r, \\ u = K\boldsymbol{x}, \end{cases} \tag{20}$$

where the system matrices are defined as

$$A := \begin{bmatrix} A_p & 0 & 0 \\ -C_p & 0 & 0 \\ 0 & 1 & 0 \end{bmatrix}, \quad B_u := \begin{bmatrix} B_p \\ 0 \\ 0 \end{bmatrix}, \quad B_r := \begin{bmatrix} 0 \\ 1 \\ 0 \end{bmatrix},$$
$$K := [K_p \;\; K_a \;\; K_b]. \tag{21}$$

For the feed drive systems, (A_p, B_p) is controllable and $C_p(sI - A_p)^{-1}B_p$ has no zero at $s = 0$, which means the augmented (A, B_u) is controllable [32]. Since the closed-loop system (20) is formulated in the standard form of the state feedback control, any design method for state feedback control can be applied, such as the pole-placement control and the linear-quadratic regulator (LQR) control. Next, the H_∞ optimization method is adopted to design the controller.

B. H_∞ OPTIMIZATION WITH PROPOSED CONTROL STRUCTURE

For the H_∞ control of feed drive systems, the performance and the control weights are introduced to tune the closed-loop performance and avoid the motor saturation. In this work, the performance weight W_p and the control weight W_u are designed as

$$z_p = W_p\boldsymbol{x}, \quad z_u = W_u u. \tag{22}$$

where z_p and z_u are the weighted outputs. The full row matrix is selected as the performance weight W_p to weigh each state of the closed-loop system (20), and the control weight W_u is designed as a scalar to adjust the control input amplitude. The generalized plant from the input r to the weighted outputs $z = [z_p \;\; z_u]^T$ is formulated as

$$\begin{cases} \dot{\boldsymbol{x}} = A\boldsymbol{x} + B_u u + B_r r, \\ z = C\boldsymbol{x} + D_u u + D_r r, \end{cases} \tag{23}$$

where the generalized matrices are

$$C = \begin{bmatrix} W_p \\ \mathbf{0} \end{bmatrix}, \quad D_u = \begin{bmatrix} 0 \\ W_u \end{bmatrix}, \quad D_r = \begin{bmatrix} 0 \\ 0 \end{bmatrix}.$$

The objective for servo control is to reduce the influence of trajectories on the weighted outputs, which means the gain of the transfer function from r to z:

$$G_{zr}(s) = (C + D_u K)(sI - (A + B_u K))^{-1}B_r \tag{24}$$

should be minimized. The H_∞ optimization can design a stabilizing state feedback controller K such that the H_∞ norm of the transfer function G_{zr} is minimized, i.e.,

$$\min \gamma \;\; s.t. \;\; \|G_{zr}\|_\infty < \gamma. \tag{25}$$

This optimization problem can be solved through the following linear matrix inequalities (LMIs) [33]:

$$\begin{bmatrix} (AX + B_u W)^T + AX + B_u W & * & * \\ {B_r}^T & -\gamma I & * \\ CX + D_u W & D_r & -\gamma I \end{bmatrix} < 0, \tag{26}$$

TABLE 1. Tuning guidelines for $W_p = [w_p\ w_v\ w_a\ w_b]$.

Weights	Trend	Step input		Ramp input error
		Speed	Overshoot	
w_p	↑	↑	↓	↓
w_v	↑	↓	↑	↑
w_a	↑	↑	↓	↓
w_b	↑	↑	↑	↑

Increase (upper-arrows); Decrease (lower-arrows).

where X is a symmetric positive definite matrix, and W is a matrix of appropriate dimension. The symbol * denotes the conjugate transpose of a matrix. By solving the LMIs (26), the feedback controller can be obtained as

$$K = WX^{-1}. \tag{27}$$

C. TUNING OF THE WEIGHTS

The steady-state error and the transient response determine the system performances. Since the zero steady-state error for the constant velocity guarantees the zero steady-state error for the position command, the steady-state error for ramp inputs and the response speed and overshoot for step inputs are considered as the main performance index of the closed-loop control system. Based on the observations, Table 1 summarizes the effects of the performance weight W_p on the index, where w_p, w_v, w_a, and w_b are corresponding components on the states p, v, x_a, and x_b, respectively.

One important tuning rule is to weigh the state of second integrator x_b more, i.e., a larger w_b, for the elimination of the tracking error at constant velocities. For the flexible model, another important principle here is that the table side states p_2 and v_2 should take more weights than the motor side states p_1 and v_1. Otherwise, the natural mode of the table cannot be well compensated.

As a summary, a simple way to tune the performance weight W_p is to set the weighting component w_b at a large value. Then, other weighting components can be tuned from low to high to specify transient performance. The tuning principle is also appropriate for the LQR controller design with the proposed control structure.

V. SIMULATION: GAIN-SCHEDULING CONTROL USING THE PARAMETER ESTIMATION FOR THE FLEXIBLE MODEL

A simulation example was conducted to verify the effectiveness of the presented online estimation and control method. In this simulation, the proposed estimator and controller were integrated for a flexible ball screw setup, which uses the estimated mass to update the gain of the state feedback controller. The designed gain-scheduling state feedback controller was compared with a linear-time-invariant state feedback controller and an adaptive backstepping sliding mode controller to verify its effectiveness.

A. CONTROLLER AND ESTIMATOR DESIGN

The ball screw setup presented in [18] was used in this simulation, of which the model parameters are given in Table 2. The

TABLE 2. Model parameters of the flexible ball screw.

Symbol	Unit	Value
b_1	Vs/rad	1.02×10^{-3}
m_1	Vs^2/rad	1.858×10^{-3}
k	V/rad	2.1002×10^{2}
c	Vs/rad	1.37×10^{-2}
b_2	Vs/rad	0
m_2	Vs^2/rad	3.79×10^{-4}

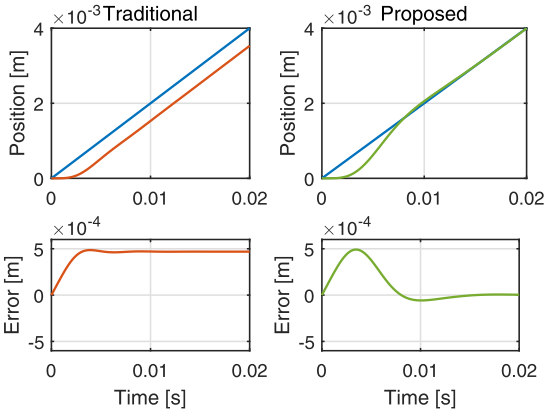

FIGURE 4. Outputs and errors of two control structures for the ramp input: ramp input (blue); traditional (orange); proposed (green).

proposed state feedback controller was designed by setting the performance and control weights as

$$\begin{cases} W_p = [w_{p_1}\ w_{p_2}\ w_{v_1}\ w_{v_2}\ w_a\ w_b] \\ \quad\ = [10^{-5}\ \ 10^{-4}\ \ 10^{-5}\ \ 5\times10^{-4}\ \ 10\ \ 10^{5}], \\ W_u = 0.0001, \end{cases}$$

and the obtained γ in (25) value was 1.046. The poles of the extended-state-observer were placed at $[-250\ \ -375\pm25i\ \ -425\ \ -500\ \ -625]$, which were far enough from the imaginary axis.

The ability of the proposed state feedback controller to eliminate the tracking error at constant velocities was verified first. As a comparison, a traditional state feedback controller with one integrator was also designed through the H_∞ optimization in Section IV-B.

Fig. 4 shows the output and the error with two controllers, and it can be seen that the traditional controller with one integrator can not achieve the zero steady-state error for the ramp input, which indicates the tracking error exists at constant velocities. Although this tracking error can be compensated by the feedforward controller, the performance is highly dependent on the model accuracy. Once the model parameters change, the effectiveness of the feedforward controller will be degraded. On the contrary, the proposed state feedback controller with double integrators well eliminate the tracking error for the ramp input.

B. PARAMETER ESTIMATION RESULTS

A jerk-limited trajectory shown in Fig. 5 was applied to the closed-loop control system, and the constant velocity and the

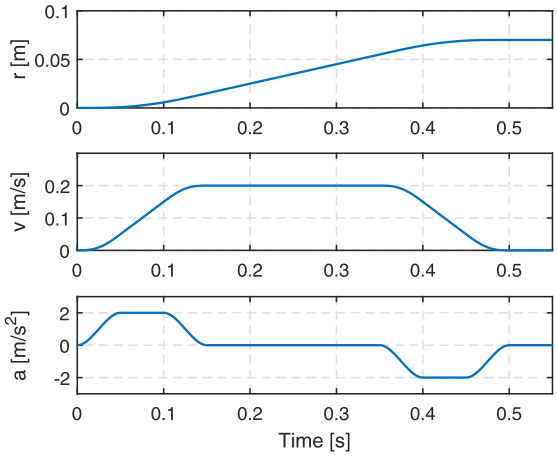

FIGURE 5. The linear trajectory for the ball screw setup.

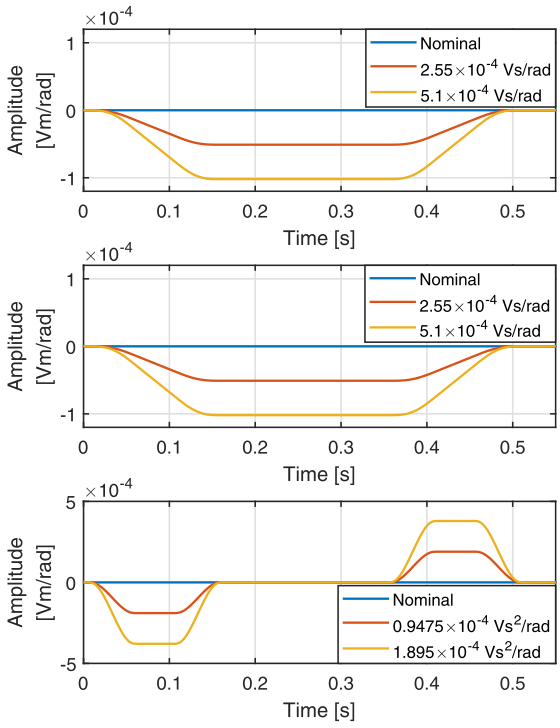

FIGURE 6. Estimated perturbations x_c for the flexible model in the presence of parameter increase: δ_{b_1} (top), δ_{b_2} (middle) and δ_{m_2} (bottom).

constant acceleration were 0.2 m/s and 2 m/s^2, respectively. As mentioned in Section II-B, the parameters b_1, b_2, and m_2 may change during manufacturing processes. When the three parameters individually varied, the estimated perturbations are shown in Fig. 6. It can be seen that the estimation for equivalent viscous friction coefficient variation was coupled with the velocity signal, while the equivalent mass variation was related to the acceleration signal.

The values of variations in the equivalent viscous friction coefficient and the equivalent mass were calculated at the constant velocity and the constant acceleration, respectively. As calculated by (11) and (12), the estimation values listed in Table 3. The results indicate that the dynamics of the

TABLE 3. Estimation values for the flexible ball screw.

Parameter and unit	Real variation	Estimation
δ_{b_1} [10^{-4}Vs/rad]	2.55	2.55
	5.1	5.1
δ_{b_2} [10^{-4}Vs/rad]	2.55	2.55
	5.1	5.1
δ_{m_2} [10^{-4}Vs^2/rad]	0.9475	0.9475
	1.895	1.895

TABLE 4. Estimation error for multiple-parameters varying cases.

Variation	δ_{b_2} 2.55×10^{-4}Vs/rad	δ_{m_2} 0.9475×10^{-4}Vs^2/rad
Only b_2	0.15%	-
Only m_2	-	0.15%
b_2 and m_2	12%	2.4%

designed extended-state-observer was fast enough to capture the parameter variations, and the observer can accurately estimate the parameter variations.

The estimation for the multiple-parameters varying case was also investigated. In this case, the sinusoidal trajectory $r = 0.01\sin(2\pi t)$ m was used. For the sinusoidal trajectory, the velocity is maximum when the acceleration is zero, and only the equivalent viscous friction coefficient affects the perturbations. Therefore, the equivalent viscous friction coefficient was estimated as (11) at maximum velocity. Similarly, the equivalent mass was estimated as (12) at maximum acceleration. Table 4 compares the estimation errors when the parameters vary individually and simultaneously. It can be seen that the estimation is very accurate when the parameters individually vary. Since the acceleration derivative was large, the estimation error was relatively larger according to (17). Although the estimation error is increased when the parameters simultaneously change, the result is still satisfactory.

C. IMPACTS OF PARAMETER VARIATIONS AND INTERPOLATING GAIN-SCHEDULING CONTROL

For flexible feed drive systems, the primary impact of parameter variations is that the control performance can be significantly deteriorated by the varying natural modes, which depends on the workpiece mass. As mentioned in [34], the table mass would increase 130% by adding 43.5 kg weight to the table. Therefore, after putting a 33.5 kg workpiece on the table, the table mass increased 100%, and the natural mode reduced from 130 Hz to 99 Hz. Fig. 7 shows the variation in the frequency response function when the load mass increases from 0 kg to 33.5 kg. Since the state feedback controller was designed as a linear time-invariant (LTI) controller without taking into account the equivalent mass variation, the stability margin, especially the gain margin, would be significantly decreased, as shown in the Nyquist plot in Fig. 8.

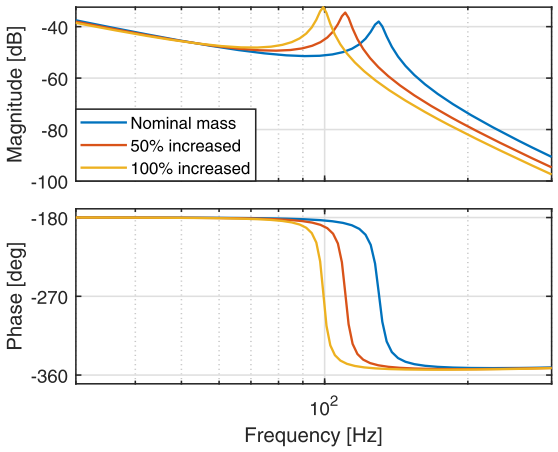

FIGURE 7. Mass-dependent natural mode.

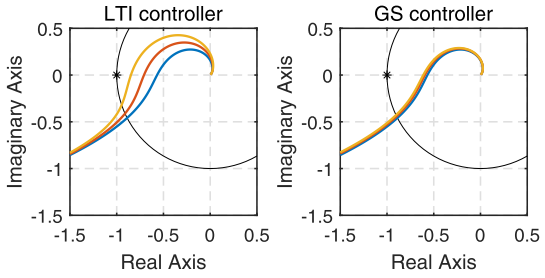

FIGURE 8. Nyquist plot: Nominal mass (blue), 25% increased (red) and 50% increased (orange).

By using the proposed parameter estimation method, the equivalent mass can be obtained in real-time, which makes it possible to update the controller using the estimated mass. In this example, two more local state feedback controllers were designed with the same weights when the mass increased by 25% and 50%. Then, a gain-scheduling (GS) controller was synthesized by linearly interpolating the gains of the three local state feedback controllers, while the estimated equivalent mass was the scheduling parameter. Note that a posteriori stability analysis for the closed-loop system under the interpolating gain-scheduling control should be conducted using the Lyapunov technique.[1] The estimation and controller update was completed during the acceleration. Nyquist plot of the designed GS controller in Fig. 8 indicates that the GS controller mitigates the stability deterioration caused by the equivalent mass variation.

The GS controller was also compared with the LTI controller in the step response test in the presence of load mass change. As shown in Fig. 9, the GS controller maintains satisfactory and consistent responses when the equivalent mass increases. However, with the LTI controller, the overshoot of the step response increased when the equivalent mass increases and the oscillations in the response reveal that the changed natural mode cannot be compensated by the LTI

[1]The Lyapunov functional technique can verify the closed-loop system stability [35], and it can guarantee the quadratic stability of linear-time-varying systems. If the constant Lyapunov function can not be found, a parameter-dependent Lyapunov function [36] can be further used.

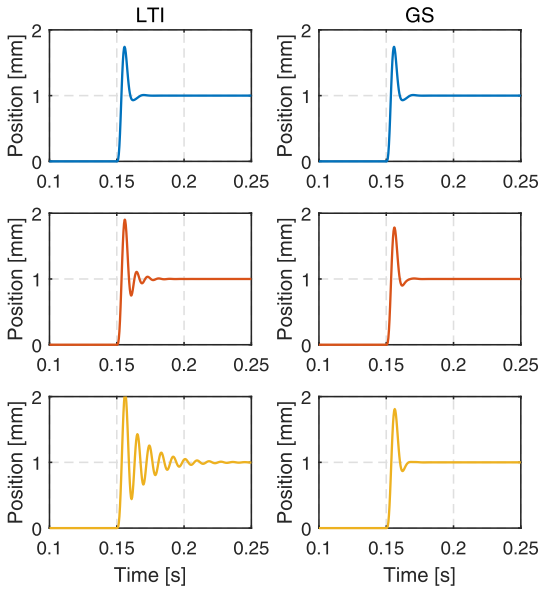

FIGURE 9. Step responses of the LTI and GS controllers: Nominal mass (blue), 25% increased (red), and 50% increased (orange).

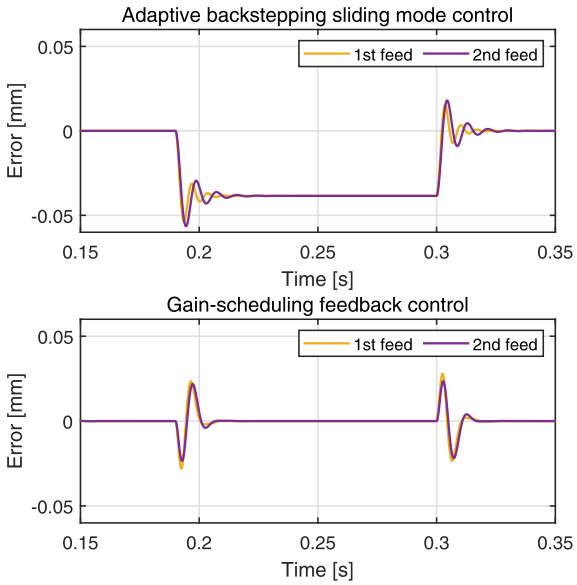

FIGURE 10. Tracking errors of ABSMC and GSFC controllers for the machining process.

controller. Even worse, it was found in simulations that the system with the LTI controller would lose stability when the equivalent mass increased 100%.

D. COMPARISON WITH ADAPTIVE BACKSTEPPING SLIDING MODE CONTROL

The GS controller was further compared with the adaptive backstepping sliding mode controller presented in [21]. In the simulated machining process, when the working table was tracking the trajectory shown in Fig. 5, the equivalent disturbance force of 0.01 V acted on the table side from 0.19 s to 0.3 s in the feed direction. The load mass changed to 16.75 kg between the first feed and the second feed.

Fig. 10 shows the tracking error before and after the mass variation. It can be seen that the designed gain-scheduling

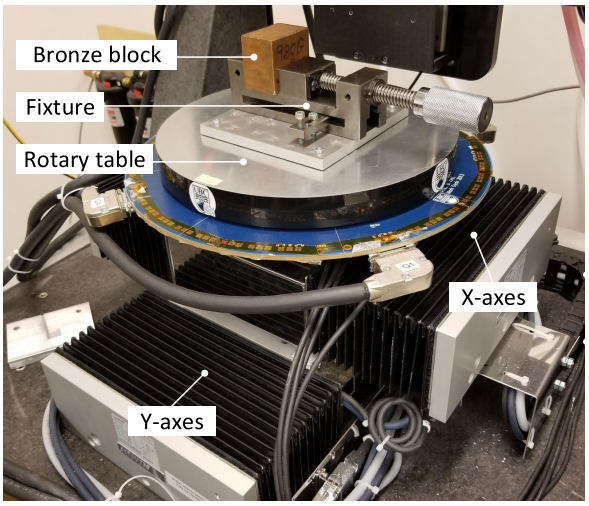

FIGURE 11. Experimental linear-motor-driven stage with different load mass.

TABLE 5. Model parameters of the linear-motor-driven stage.

Symbol	Unit	Axis	
		X	Y
K_t	N/V	45.4	72.5
b	Vs/m	0.5518	0.2834
m	Vs^2/m	0.4007	0.8161

* K_t is the motor force constant.

state feedback controller yields more consistent and smooth responses in the presence of the mass variation. On the contrary, the tracking error of the adaptive backstepping sliding mode controller changed after the mass variation. Furthermore, the adaptive backstepping sliding mode controller can not wholly reject the disturbance force, since the tracking error significantly increased between 0.19 s and 0.3 s. The results indicate that, by using the estimated parameter to schedule the proposed state feedback controller with double integrators, the obtained gain-scheduling controller outperformed the adaptive backstepping sliding mode controller in the presence of the unmeasurable mass variation.

VI. EXPERIMENT ON A LINEAR-MOTOR-DRIVEN STAGE

The proposed parameter estimator and state feedback controller were experimentally applied to a linear-motor-driven X-Y stage shown in Fig. 11. This setup is driven by two axes, which can be commonly modeled as the rigid model, and the model parameters in (7) are listed in Table 5. The remaining rotary table, fixture and bronze block were used to change the equivalent mass. Since the variation in the equivalent viscous friction coefficient in this setup is not apparent, only the estimation for the equivalent mass will be presented.

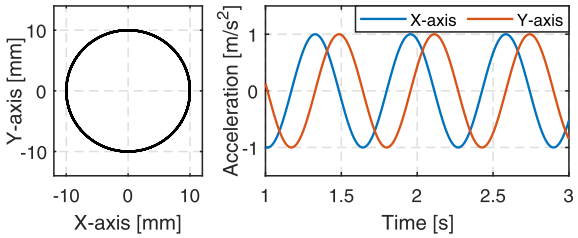

FIGURE 12. Profile and acceleration of the circular trajectory.

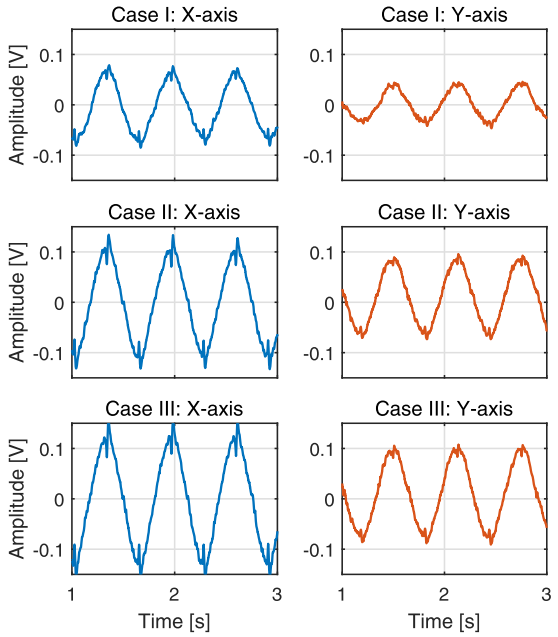

FIGURE 13. Estimated perturbation x_c for three cases.

A. CONTROLLER AND ESTIMATOR DESIGN

By tuning the weight as $W_p = [1 \quad 0.1 \quad 10^3 \quad 5 \times 10^5]$ and $W_u = 0.0001$, the state feedback controller for X-axis and Y-axis was respectively obtained as

$$K_X = \left[1.48\times10^8 \quad 6.30\times10^4 \quad -2.84\times10^{10} \quad -3.63\times10^{12}\right],$$
$$K_Y = \left[9.93\times10^7 \quad 6.89\times10^4 \quad -1.86\times10^{10} \quad -2.29\times10^{12}\right]. \tag{28}$$

The system bandwidth under obtained controllers for X-axis and Y-axis is 326 rad/s and 330 rad/s, respectively. According to the estimator parameterization for the rigid model (18), the tuning parameters of L were designed as

$$L = \left[9\times10^5 \quad 2.7\times10^8 \quad 2.7\times10^{10}\right]^T. \tag{29}$$

As shown in Fig. 12, a circular trajectory with a maximum acceleration of 1 m/s^2 was applied to the driven stage, and on each axis, the velocity and the acceleration were sinusoidal. Given the circle trajectory, if the equivalent viscous friction coefficient varied, it could be estimated when the acceleration is zero. On the other hand, the equivalent mass variation was estimated when the velocity is zero (acceleration is maximum) in this case.

TABLE 6. Experimental results of linear motor stage.

Load	Weight $[kg]$	Estimation $[kg]$		Estimation error	
		x	y	x	y
1	2.95	2.95	2.78	0%	5.8%
2	5.08	4.72	5.31	7.1%	4.5%
3	5.98	5.59	6.24	6.5%	4.4%

B. EXPERIMENTAL RESULTS

As shown in Fig. 11, a rotary table, a fixture, and a bronze block were used as weights to change the equivalent mass. Three cases of the parameter variations were considered in the experiment:

- Case I, only rotary table.
- Case II, rotary table and fixture.
- Case III, rotary table, fixture and bronze block.

The mass of each case is listed in Table 6.

Since the setup is a two-axes stage, both X-axis and Y-axis can be used to estimate the change of equivalent mass. Fig. 13 shows the estimated perturbation $\boldsymbol{x}_c$ caused by the mass change. It can be seen that the estimated perturbation varies with the acceleration. The maximum acceleration was used to calculate the mass of load weights. According to (12), the estimation results are listed in Table 6, which indicates that the parameter variations can be effectively estimated.

VII. CONCLUSION

In this paper, a significant problem caused by the parameter variations in feed drive systems was overcome by proposing a novel method of online estimation and control. The core concept of the proposed parameter estimation method is regarding the perturbations caused by the parameter variations as the extended states, formulating a new system containing the extended states, and estimating the extended states through the observer. A state feedback control structure with double integrators was further proposed for achieving zero tracking error at constant velocities. The controller was designed through the H_∞ optimization, and the tuning guidelines for the proposed state feedback control were also given. Furthermore, since the proposed state feedback controller was formulated in the standard form, it can also be designed through the existing methods, such as pole-placement control and LQR control.

To handle the impacts of parameter variations on the control performance, the estimated parameter was used as the scheduling parameter to schedule the gain of the proposed state feedback controller. The results indicate that the proposed online estimation and control could be useful in manufacturing products with feed drives in high and uniform precision.

REFERENCES

[1] Y. Altintas, A. Verl, C. Brecher, L. Uriarte, and G. Pritschow, "Machine tool feed drives," *CIRP Ann.-Manuf. Technol.*, vol. 60, no. 2, pp. 779–796, 2011.

[2] A. H. H. Hosseinabadi and Y. Altintas, "Modeling and active damping of structural vibrations in machine tools," *CIRP J. Manuf. Sci. Technol.*, vol. 7, no. 3, pp. 246–257, 2014.

[3] D. J. Gordon and K. Erkorkmaz, "Accurate control of ball screw drives using pole-placement vibration damping and a novel trajectory prefilter," *Precis. Eng.*, vol. 37, no. 2, pp. 308–322, Apr. 2013.

[4] A. Dumanli and B. Sencer, "Optimal high-bandwidth control of ball-screw drives with acceleration and jerk feedback," *Precis. Eng.*, vol. 54, pp. 254–268, Oct. 2018.

[5] Z. Sun, P. Zahn, A. Verl, and A. Lechler, "A new control principle to increase the bandwidth of feed drives with large inertia ratio," *Int. J. Adv. Manuf. Technol.*, vol. 91, nos. 5–8, pp. 1747–1752, Jul. 2017.

[6] M. Hanifzadegan and R. Nagamune, "Switching gain-scheduled control design for flexible ball-screw drives," *J. Dyn. Syst., Meas., Control*, vol. 136, no. 1, Jan. 2014.

[7] C. Zhang and Y. Chen, "Tracking control of ball screw drives using ADRC and equivalent-error-model-based feedforward control," *IEEE Trans. Ind. Electron.*, vol. 63, no. 12, pp. 7682–7692, Dec. 2016.

[8] D. Sepasi, R. Nagamune, and F. Sassani, "Tracking control of flexible ball screw drives with runout effect and mass variation," *IEEE Trans. Ind. Electron.*, vol. 59, no. 2, pp. 1248–1256, Feb. 2012.

[9] M. Hanifzadegan and R. Nagamune, "Tracking and structural vibration control of flexible ball–screw drives with dynamic variations," *IEEE/ASME Trans. Mechatronics*, vol. 20, no. 1, pp. 133–142, Feb. 2015.

[10] L. Dong, W. Tang, and D. Bao, "Interpolating gain-scheduled H∞ loop shaping design for high speed ball screw feed drives," *ISA Trans.*, vol. 55, pp. 219–226, Mar. 2015.

[11] W. Symens, H. van Brussel, and J. Swevers, "Gain-scheduling control of machine tools with varying structural flexibility," *CIRP Ann.-Manuf. Technol.*, vol. 53, no. 1, pp. 321–324, 2004.

[12] H. Liu, J. Zhang, and W. Zhao, "An intelligent non-collocated control strategy for ball-screw feed drives with dynamic variations," *Engineering*, vol. 3, no. 5, pp. 641–647, Oct. 2017.

[13] M. Karkoub, G. Balas, K. Tamma, and M. Donath, "Robust control of flexible manipulators via μ-synthesis," *Control Eng. Pract.*, vol. 8, no. 7, pp. 725–734, Jul. 2000.

[14] P. Apkarian and R. J. Adams, "Advanced gain-scheduling techniques for uncertain systems," in *Advances in Linear Matrix Inequality Methods in Control*. Philadelphia, PA, USA: SIAM, 2000, pp. 209–228.

[15] B. Yao, M. Al-Majed, and M. Tomizuka, "High-performance robust motion control of machine tools: An adaptive robust control approach and comparative experiments," *IEEE/ASME Trans. Mechatronics*, vol. 2, no. 2, pp. 63–76, Jun. 1997.

[16] J. Yao, Z. Jiao, and D. Ma, "Adaptive robust control of DC motors with extended state observer," *IEEE Trans. Ind. Electron.*, vol. 61, no. 7, pp. 3630–3637, Jul. 2014.

[17] T. Beauduin, H. Fujimoto, and Y. Terada, "Adaptive vibration suppression perfect tracking control for linear time-varying systems with application to ball-screw feed drives," in *Proc. IEEE 14th Int. Workshop Adv. Motion Control (AMC)*, Apr. 2016, pp. 245–250.

[18] K. Erkorkmaz and A. Kamalzadeh, "High bandwidth control of ball screw drives," *CIRP Ann.-Manuf. Technol.*, vol. 55, no. 1, pp. 393–398, 2006.

[19] A. Kamalzadeh and K. Erkorkmaz, "Compensation of axial vibrations in ball screw drives," *CIRP Ann.-Manuf. Technol.*, vol. 56, no. 1, pp. 373–378, 2007.

[20] C. Okwudire and Y. Altintas, "Minimum tracking error control of flexible ball screw drives using a discrete-time sliding mode controller," *J. Dyn. Syst., Meas., Control*, vol. 131, no. 5, Sep. 2009, Art. no. 051006.

[21] L. Dong and W. C. Tang, "Adaptive backstepping sliding mode control of flexible ball screw drives with time-varying parametric uncertainties and disturbances," *ISA Trans.*, vol. 53, no. 1, pp. 110–116, Jan. 2014.

[22] A. Kamalzadeh and K. Erkorkmaz, "Accurate tracking controller design for high-speed drives," *Int. J. Mach. Tools Manuf.*, vol. 47, no. 9, pp. 1393–1400, Jul. 2007.

[23] H. Fujimoto and T. Takemura, "High-precision control of ball-screw-driven stage based on repetitive control using *n*-times learning filter," *IEEE Trans. Ind. Electron.*, vol. 61, no. 7, pp. 3694–3703, Jul. 2014.

[24] Y.-R. Pan, Y.-T. Shih, R.-H. Horng, and A.-C. Lee, "Advanced parameter identification for a linear-motor-driven motion system using disturbance observer," *Int. J. Precis. Eng. Manuf.*, vol. 10, no. 4, pp. 35–47, Oct. 2009.

[25] W.-S. Huang, C.-W. Liu, P.-L. Hsu, and S.-S. Yeh, "Precision control and compensation of servomotors and machine tools via the disturbance observer," *IEEE Trans. Ind. Electron.*, vol. 57, no. 1, pp. 420–429, Jan. 2010.

[26] C. Yang, Y. Jiang, W. He, J. Na, Z. Li, and B. Xu, "Adaptive parameter estimation and control design for robot manipulators with finite-time convergence," *IEEE Trans. Ind. Electron.*, vol. 65, no. 10, pp. 8112–8123, Oct. 2018.
[27] S. Li, J. Yang, W.-C. Chen, and X. Chen, "Generalized extended state observer based control for systems with mismatched uncertainties," *IEEE Trans. Ind. Electron.*, vol. 59, no. 12, pp. 4792–4802, Dec. 2012.
[28] J. Han, "From PID to active disturbance rejection control," *IEEE Trans. Ind. Electron.*, vol. 56, no. 3, pp. 900–906, Mar. 2009.
[29] J. Liu, Y. Gu, L. Zha, Y. Liu, and J. Cao, "Event-triggered H_∞ load frequency control for multiarea power systems under hybrid cyber attacks," *IEEE Trans. Syst., Man, Cybern., Syst.*, vol. 49, no. 8, pp. 1665–1678, Aug. 2019.
[30] A. Alizadegan, P. Zhao, R. Nagamune, and M. Chiao, "Robust H_∞ control of miniaturized optical image stabilizers against product variabilities," *Control Eng. Pract.*, vol. 80, pp. 70–82, 2018.
[31] Z. Gao, "Scaling and bandwidth-parameterization based controller tuning," in *Proc. Amer. Control Conf.*, vol. 6, Apr. 2006, pp. 4989–4996.
[32] C. Chen, *Linear System Theory and Design* (Oxford Series in Electrical and Computer Engineering). London, U.K.: Oxford Univ. Press, 2013.
[33] G. Duan and H. Yu, *LMIs in Control Systems: Analysis, Design and Applications*. Boca Raton, FL, USA: CRC Press, 2013.
[34] A. Kamalzadeh, D. J. Gordon, and K. Erkorkmaz, "Robust compensation of elastic deformations in ball screw drives," *Int. J. Mach. Tools Manuf.*, vol. 50, no. 6, pp. 559–574, Jun. 2010.
[35] K. Wang, E. Tian, J. Liu, L. Wei, and D. Yue, "Resilient control of networked control systems under deception attacks: A memory-event-triggered communication scheme," *Int. J. Robust. Nonlinear Control*, vol. 30, pp. 1534–1548, 2020.
[36] P. Gahinet, P. Apkarian, and M. Chilali, "Affine parameter-dependent Lyapunov functions and real parametric uncertainty," *IEEE Trans. Autom. Control*, vol. 41, no. 3, pp. 436–442, Mar. 1996.

TIANCHENG ZHONG received the B.S. degree from Southeast University, Nanjing, China, in 2014, where he is currently pursuing the Ph.D. degree.

From September 2017 to August 2019, he was a visiting Ph.D. student at the Department of Mechanical Engineering, The University of British Columbia, Vancouver, BC, Canada. His research interests include robust control, gain-scheduling control, data-driven control, and their applications to feed drive systems.

RYOZO NAGAMUNE (Senior Member, IEEE) received the B.S. and M.S. degrees in control engineering from Osaka University, Suita, Japan, in 1995 and 1997, respectively, and the Ph.D. degree in applied mathematics from the Royal Institute of Technology, Stockholm, Sweden, in 2002.

He has been with the Department of Mechanical Engineering, The University of British Columbia, Vancouver, BC, Canada, since 2006, where he is currently an Associate Professor. His current research interest includes robust control theory and applications to mechatronic systems.

Dr. Nagamune is the Chair of the IEEE Joint Chapter of Control Systems, Robotics, and Automation, and Systems, Man, and Cybernetics Societies in Vancouver Section. He held the Canada Research Chair, Tier 2, in control engineering, from 2013 to 2018.

ALEXANDER YUEN received the bachelor's, master's, and Ph.D. degrees from The University of British Columbia, Vancouver, BC, Canada, in 2011, 2013, and 2018, respectively, all in applied science.

He is currently working as a Vehicle Controls and Dynamics Engineer at Hyperloop One.

WENCHENG TANG received the B.S., M.S., and Ph.D. degrees from Southeast University, Nanjing, China, in 1982, 1987, and 2003, respectively.

Since 1982, he has been with the School of Mechanical Engineering, Southeast University, where he is currently a Professor. His main research interests are CAD/CAE/CAM, computer integrated manufacturing, and structural optimization.